



Iron “ore” nothing: benthic iron fluxes from the oxygen-deficient Santa Barbara Basin enhance phytoplankton productivity in surface waters

De'Marcus Robinson¹, Anh L. D. Pham¹, David J. Yousavich², Felix Janssen^{3,4}, Frank Wenzhöfer^{3,4}, Eleanor C. Arrington⁵, Kelsey M. Gosselin⁶, Marco Sandoval-Belmar¹, Matthew Mar¹, David L. Valentine⁵, Daniele Bianchi¹, and Tina Treude^{1,2}

¹Department of Atmospheric and Oceanic Sciences, University of California Los Angeles, Los Angeles, CA, USA

²Department of Earth, Planetary, and Space Sciences, University of California Los Angeles, Los Angeles, CA, USA

³HGF-MPG Joint Research Group for Deep-Sea Ecology and Technology, Alfred Wegener Institute, Helmholtz Centre for Polar and Marine Research, Bremerhaven, Germany

⁴HGF-MPG Joint Research Group for Deep-Sea Ecology and Technology, Max Planck Institute for Marine Microbiology, Celsiusstraße 1, 28359 Bremen, Germany

⁵Department of Earth Science and Marine Science Institute, University of California, Santa Barbara, CA 93106, USA

⁶Interdepartmental Graduate Program in Marine Science, University of California, Santa Barbara, CA 93106, USA

Correspondence: De'Marcus Robinson (demarcus1.robinson@atmos.ucla.edu) and Tina Treude (ttreude@g.ucla.edu)

Received: 9 December 2022 – Discussion started: 14 December 2022

Revised: 31 October 2023 – Accepted: 28 November 2023 – Published: 14 February 2024

Abstract. The trace metal iron (Fe) is an essential micronutrient that controls phytoplankton productivity, which subsequently affects organic matter cycling with feedback on the cycling of macronutrients. Along the continental margin of the US West Coast, high benthic Fe release has been documented, in particular from deep anoxic basins in the Southern California Borderland. However, the influence of this Fe release on surface primary production remains poorly understood. In the present study from the Santa Barbara Basin, in situ benthic Fe fluxes were determined along a transect from shallow to deep sites in the basin. Fluxes ranged between 0.23 and 4.9 mmol m⁻² d⁻¹, representing some of the highest benthic Fe fluxes reported to date. To investigate the influence of benthic Fe release from the oxygen-deficient deep basin on surface phytoplankton production, we combined benthic flux measurements with numerical simulations using the Regional Ocean Modeling System coupled to the Biogeochemical Elemental Cycling (ROMS-BEC) model. For this purpose, we updated the model Fe flux parameterization to include the new benthic flux measurements from the Santa Barbara Basin. Our simulations suggest that benthic Fe fluxes enhance surface primary production, supporting a

positive feedback on benthic Fe release by decreasing oxygen in bottom waters. However, a reduction in phytoplankton Fe limitation by enhanced benthic fluxes near the coast may be partially compensated for by increased nitrogen limitation further offshore, limiting the efficacy of this positive feedback.

1 Introduction

The California Current System (CCS), located off the coasts of Washington, Oregon, and California, is a typical eastern boundary upwelling system, where seasonal upwelling supports a highly diverse and productive marine ecosystem (Chavez and Messié, 2009; Carr and Kearns, 2003). The CCS can be split into three main parts: the main equatorward California Current offshore, a subsurface poleward undercurrent fringing the continental shelf, and a recirculation pattern known as the Southern California Eddy in the Southern California Bight.

In the CCS, both upwelling and large-scale circulation provide essential nutrients to the euphotic zone, where they

fuel high rates of net primary production (NPP). While seasonal upwelling dominates north of Point Conception, advection by the CCS provides a major route for nutrient supply to the Santa Barbara Channel in the Southern California Bight (Bray et al., 1999). Following phytoplankton blooms, sinking and degradation of organic matter lead to oxygen consumption and widespread oxygen loss in subsurface waters (Brander et al., 2017; Chavez and Messié, 2009). Along the southern California coast, this oxygen depletion is exacerbated by regional circulation patterns that include transport of low-oxygen waters of tropical origin along the poleward undercurrent (Evans et al., 2020; Pozo Buil and Di Lorenzo, 2017). Oxygen decline is particularly apparent in deep, isolated basins such as those found in the southern California continental borderland, where the presence of shallow sills limits ventilation of deep waters, and anoxic conditions are often encountered near the bottom (Reimers et al., 1990; Goericke et al., 2015; White et al., 2019).

In the CCS, the trace metal iron (Fe) has been identified as a limiting factor for the growth of phytoplankton (Hogle et al., 2018). Fe is an essential micronutrient that also has a considerable influence on the dynamics of phosphorus and nitrogen in the euphotic zone (Tagliabue et al., 2017). Similar to other nutrients, Fe is transported to the surface by upwelling and circulation. However, Fe supply is generally low in oxygenated environments relative to other macronutrients, reflecting rapid scavenging of insoluble iron-oxide minerals by sinking particles that eventually accumulate in the sediment (Bruland et al., 2001, 2014; Firme et al., 2003; Till et al., 2019). While early studies suggested that Fe inputs to the CCS are dominated by rivers and aeolian deposition (Billler and Bruland, 2013; Johnson et al., 2003), more recent work highlights a combination of sources, including benthic fluxes (Severmann et al., 2010; Noffke et al., 2012; Tagliabue et al., 2017; Wallmann et al., 2022) and ocean currents, which help redistribute Fe in coastal waters (Bray et al., 1999; Boiteau et al., 2019; García-Reyes and Largier, 2010).

Benthic release of Fe(II), the reduced and soluble form of Fe, has been recognized as a potential source of Fe to the surface ocean along the continental shelf and slope of the CCS, including the deep basins of the California borderland (John et al., 2012; Severmann et al., 2010). Under hypoxic or anoxic bottom waters, Fe(II) produced in the sediment during microbial organic matter degradation coupled to Fe(III) reduction diffuses across the sediment–water interface and accumulates in the water column (Furrer and Wehrli, 1993; Dale et al., 2015; Severmann et al., 2010; Wallmann et al., 2022). In the CCS, this benthic Fe flux is likely to exceed atmospheric deposition (Deutsch et al., 2021) and may ultimately make its way to the surface by upwelling and vertical mixing, supporting high rates of photosynthesis.

The interaction among low bottom water oxygen, Fe(II) release, and transport by the ocean circulation is particularly important in the Santa Barbara Basin (SBB), an oxygen-deficient basin located between the Channel Islands and

mainland California in the Southern California Bight. The SBB frequently experiences seasonal anoxia in the bottom water in fall, with irregular oxygen flushing of dense, hypoxic water below the western sill depth (470 m) during winter and spring (Goericke et al., 2015; Sholkovitz and Soutar, 1975; White et al., 2019; Qin et al., 2022). This seasonal flushing reflects either changes in upwelling strength and frequency or changes in stratification at the sill depth, although the exact cause of the flushing is still unclear (Goericke et al., 2015; Sholkovitz and Gieskes, 1971; White et al., 2019). Lack of oxygen in the deeper parts of the basin supports anaerobic microbial processes in the bottom water and sediment (White et al., 2019), including benthic Fe reduction (Goericke et al., 2015), causing the release of Fe(II) into the water column (Severmann et al., 2010). Ventilation events that re-oxygenate the deep basin, as well as mixing by the vigorous submesoscale circulation (Kessouri et al., 2020), could allow upwelling of this Fe above the sill depth and ultimately to the surface, providing a linkage between benthic processes and upper water-column biogeochemistry. Increased surface primary production supported by this Fe source would in turn drive higher remineralization and oxygen loss in deep waters, thus providing a positive feedback to benthic Fe release. However, with a dearth of benthic Fe flux measurements in the SBB, gaps remain in our understanding of the dynamics and impact of benthic Fe flux in the Southern California Borderland, particularly with respect to its magnitude, dependence on bottom water oxygen, and ability to reach the euphotic zone and influence primary production.

In this study, we explore the connection between benthic Fe flux and surface primary production in the CCS by investigating the influence of enhanced benthic Fe fluxes from low-oxygen waters with a combination of field observations and experiments with a numerical model. We focus on the SBB, where we provide a new set of benthic Fe flux estimates determined by in situ benthic flux chamber measurements. We combine these new observations with existing data (Severmann et al., 2010) to revise the representation of benthic Fe fluxes in UCLA’s Regional Ocean Modeling System coupled to the Biogeochemical Elemental Cycling (ROMS-BEC) model (Deutsch et al., 2021). We then use the model to evaluate the effect of benthic Fe fluxes on surface nutrient consumption and NPP and compare their impact to that of aeolian Fe deposition in the SBB and beyond.

2 Materials and methods

2.1 Study site

Fieldwork in the SBB was conducted between 29 October and 11 November 2019, during the R/V *Atlantis* cruise AT42-19. Sampling occurred during the anoxic, non-upwelling season along one bimodal transect with six stations in total at depths between 447 and 585 m (Fig. 1, Table 1).

Table 1. Station details and geochemical parameters determined during the AT42-19 expedition. Benthic Fe fluxes were determined using in situ benthic chambers. Dissolved O₂ concentrations were measured in the water column at 10 m above the seafloor using a Sea-Bird optode sensor attached to the ROV *Jason*. At stations with two benthic chamber deployments (NDT3A and SDRO), O₂, geographical coordinates, and depth were averaged as there were only minimal differences between the two chamber deployments.

Station	Fe Flux [mmol m ⁻² d ⁻¹]	O ₂ [mmol m ⁻³]	Latitude [° N]	Longitude [° E]	Depth [m]
NDT3C	0.23 (<i>n</i> = 1)	5.3	34.3526	120.0160	499
NDT3B	0.36 (<i>n</i> = 1)	6.8	34.3336	120.0188	535
NDT3A	1.73; 1.20 (<i>n</i> = 2)	9.6	34.2921	120.0258	572
NDRO	3.49 (<i>n</i> = 1)	0.0	34.2618	120.0309	581
SDRO	4.90; 3.92 (<i>n</i> = 2)	0.0	34.2011	120.0446	586
SdT3D	0.58 (<i>n</i> = 1)	9.6	34.1422	120.0515	446

Transects were divided into northern (Northern Depocenter Transect Three, NDT3) and southern (Southern Depocenter Transect Three, SDT3) sites based on basin geography (Fig. 1). Stations were labeled alphabetically from A (deepest) to D (shallowest) according to their location along the transect, except for the deepest stations at the bottom of the basin, which were labeled Northern Depocenter Radial Origin (NDRO) and Southern Depocenter Radial Origin (SDRO).

2.2 Benthic flux chambers

Custom-built cylindrical benthic flux chamber systems (Treude et al., 2009) were deployed by the ROV *Jason* at the six stations (Fig. 1). Polycarbonate chambers (19 cm inner diameter) were installed in a small lightweight frame made from fiber-reinforced plastics. A stirrer (Type K/MT 111, K.U.M. Umwelt- und Meerestechnik, Kiel, Germany) was used to keep the water overlying the sediment enclosed by the chamber well mixed. One or two replicate chamber systems were deployed at each site. Since sediment in the SBB is quite soft and poorly consolidated, especially towards the deeper stations, frames were fitted with platforms attached to the feet of the frame and with buoyant syntactic foam to reduce sinking into the sediment. A syringe sampler was equipped with six glass sampling syringes that were connected with 50 cm long plastic tubes (2.5 mm inner diameter, Vygon, Aachen, Germany). Each sampling syringe withdrew 50 mL of the overlying seawater at pre-programmed times. A seventh syringe was used to inject 50 mL of de-ionized water shortly after chambers were deployed to calculate chamber volume from the salinity drop recorded with a conductivity sensor (type 5860, Aanderaa Data Instruments, Bergen, NO) in the overlying water, following the approach described in Kononets et al. (2021). Water samples were analyzed for Fe(II) on the ship using a Shimadzu UV spectrophotometer (UV-1800), equipped with a sipper unit, following the procedure of Grasshoff et al. (1999). Fe fluxes were calculated from the slope of linear fits of Fe concentration time series vs. time (Fig. S1 in the Supplement), multiplied by the cham-

ber volume and divided by the surface area of the sediment (Kononets et al., 2021).

2.3 Numerical model (ROMS-BEC)

To explore the impacts of benthic Fe fluxes on surface primary production, we used a well-established ocean biogeochemical model of the CCS (Renault et al., 2016; Deutsch et al., 2021). The physical model component consists of the Regional Ocean Modeling System (ROMS) (Shchepetkin, 2015; Shchepetkin and McWilliams, 2005), a primitive-equation, hydrostatic, topography-following ocean model. As in prior work, the model domain spans the entire US West Coast, from Baja California to Vancouver Island, with a horizontal resolution of 4 km, enough to resolve the mesoscale circulation (Capet et al., 2008). The baseline model configuration was run over the 1995–2017 period with interannually varying atmospheric forcings. We refer the reader to earlier publications (Renault et al., 2021; Deutsch et al., 2021) for a complete description of the model configuration, setup, forcings, and boundary conditions used in this study.

ROMS is coupled online to the Biogeochemical Elemental Cycling (BEC) model (Moore et al., 2004), adapted for the US West Coast by Deutsch et al. (2021). BEC solves the equations for the evolution of six nutrients (nitrate (NO₃⁻), ammonium (NH₄⁺), nitrite (NO₂⁻), silicate (SiO₂), phosphate (PO₄³⁻), and iron (Fe)), three phytoplankton groups (small phytoplankton, diatoms, and diazotrophs), a single zooplankton group, inorganic carbon, oxygen (O₂), and dissolved organic matter (carbon, nitrogen, phosphorus, and iron). Nutrient and carbon cycles are coupled by a fixed stoichiometry, except for silica and Fe, which use variable stoichiometries (Deutsch et al., 2021; Moore et al., 2001, 2004). The Fe cycle in BEC includes four separate pools: dissolved inorganic Fe (dFe), dissolved and particulate organic Fe, and Fe associated with mineral dust. Of these, only dissolved organic and inorganic Fe are explicitly tracked as state variables, while particulate Fe is treated implicitly by resolving vertical-sinking particle fluxes (Moore et al., 2001; Moore and Braucher, 2008). Four main processes control the cycle

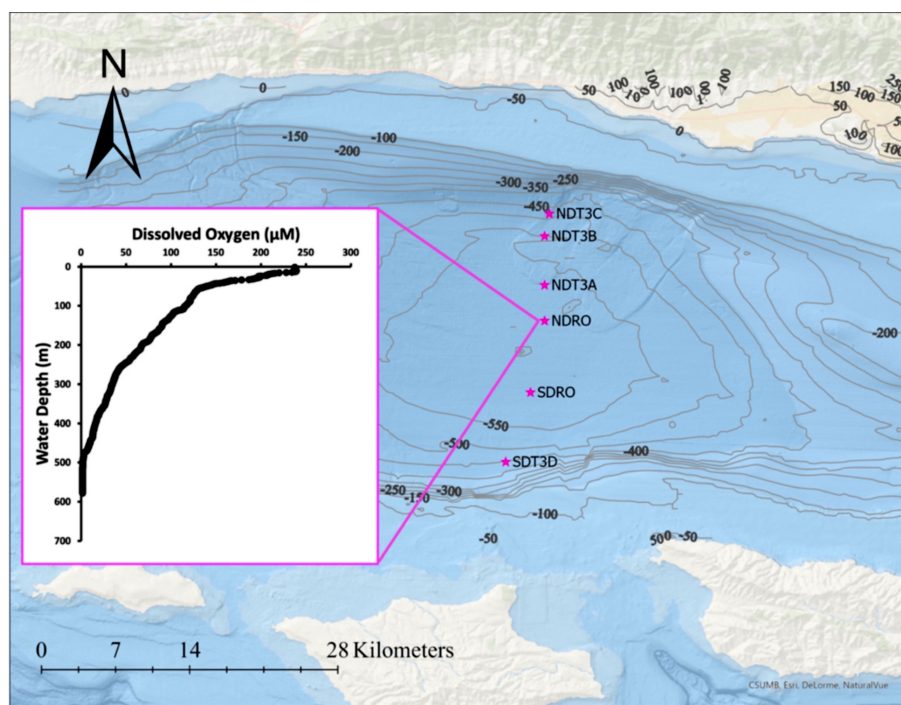


Figure 1. Station locations in the SBB during the AT42-19 expedition with R/V *Atlantis*. NDT3 (with stations A, B, and C): Northern Depocenter Transect Three, NDRO: Northern Depocenter Radial Origin, SDRO: Southern Depocenter Radial Origin, SDT3 (with station D): Southern Depocenter Transect Three. The small insert figure displays dissolved oxygen concentrations in the water column at the NDRO station profiled by an optical oxygen sensor attached to the AUV *Sentry*. The profile was measured at the following position: latitude 34.2618° N, longitude 120.0309° E. The map was created using ArcGIS Ocean Basemap, with bathymetric contour lines representing depth information taken from the General Bathymetric Chart of the Oceans (GEBCO) database.

of Fe in the model: atmospheric deposition, biological uptake and remineralization, scavenging by sinking particles, and release by sediment. The atmospheric dFe deposition is based on the dust climatology of Mahowald et al. (2006) and dissolution rates from Moore and Braucher (2008). Different from Deutsch et al. (2021), we re-evaluated the dependence of benthic dFe fluxes on bottom water O_2 concentrations in the California margin based on a merged dataset that combines our measurements from the SCB with those presented in Sevmann et al. (2010) (see Sect. 2.5). The model Fe scavenging scheme removes dFe from the water column at a rate proportional to sinking particle fluxes and dFe concentrations, assuming a uniform concentration of 0.6 nM of Fe-binding ligands (Moore et al., 2004; Moore and Braucher, 2008). Accordingly, scavenging rates increase strongly at dFe concentrations greater than 0.6 nM, and, vice versa, rates decrease strongly below 0.5 nM (Fig. S2). Note that, while simplistic, this formulation is still widely adopted by global ocean biogeochemistry models (Tagliabue et al., 2014, 2016), although improvements have been proposed (Moore and Braucher, 2008; Aumont et al., 2015; Pham and Ito, 2019, 2018).

As shown in previous work, the model captures the main patterns of physical and biogeochemical variability in the CCS, providing a representation of nutrient cycles and NPP

in good agreement with observations (Renault et al., 2021; Deutsch et al., 2021). We further evaluate the model against an extended set of dissolved Fe measurements for the CCS (see Sects. 2.4 and 3.1).

2.4 Fe dataset along the US West Coast

To assess the ability of the model to capture observed patterns in dFe along the US West Coast, we gathered available dFe concentration measurements from published studies, including a global compilation (Tagliabue et al., 2016); regional programs such as the California Cooperative Oceanic Fisheries Investigations (CalCOFI), CCE-LTER, IRNBRU, and MBARI cruises (Bundy et al., 2016; Hogle et al., 2018; Johnson et al., 2003; King and Barbeau, 2011); and other individual studies (Billler and Bruland, 2013; Boiteau et al., 2019; Bundy et al., 2014, 2015, 2016; Chappell et al., 2019; Chase, 2002; Chase et al., 2005; Firme et al., 2003; Hawco et al., 2021; John et al., 2012; Till et al., 2019). In the final compilation, we define dFe as the sum of the dissolved Fe and dissolvable Fe, based on the definitions used in each publication. Different studies used different filter sizes to define the dFe pool, most commonly 0.20, 0.40, and 0.45 μ m, and different sampling methods, such as bottles, pump systems, and/or surface tows. In some studies, samples were briefly

acidified before being analyzed. Despite the differences in sampling and measurement approaches, we found that these datasets generally agreed with each other, suggesting that the final compilation accurately represents the dFe distribution along the US West Coast. The final dataset includes observations from 1980 to 2021, with most samples collected between 1997 and 2015, and from the upper 100 m of the water column.

2.5 Experimental design

To evaluate the impact of Fe fluxes from low- O_2 sediment in the SBB on surface biogeochemistry, we designed a suite of model sensitivity experiments with ROMS-BEC in which external sources of Fe are modified relative to a baseline simulation. Accordingly, we run the following model experiments.

High flux. This experiment is the baseline model simulation, using an Fe flux parameterization calculated as an exponential fit to a dataset of benthic Fe fluxes consisting of the new benthic measurements from AT42-19 and previous observations from the US West Coast (Severmann et al., 2010) (see Sect. 3.2), thus updating the parameterization by Deutsch et al. (2021). Benthic Fe release follows the following equation:

$$\log_{10}(\text{Fe}) = 2.86 - 0.01 \cdot O_2, \quad (1)$$

where O_2 is the concentration of oxygen in mmol m^{-3} , and (Fe) is the Fe flux in $\mu\text{mol m}^{-2} \text{d}^{-1}$. This revised formulation is only applied in the SBB where we performed our measurements, while a different formulation, solely based on data by Severmann et al. (2010), is used outside of the SBB:

$$\log_{10}(\text{Fe}) = 2.6178 - 0.0128 O_2. \quad (2)$$

For this parameterization, we corrected a model bias that resulted in modeled bottom O_2 concentrations greater than 30 mmol m^{-3} over most of the deep basins where observations indicated lower concentrations down to oxygen-free conditions (Fig. S3). We therefore reduced modeled bottom water O_2 concentrations in the Southern California Borderland by 30 mmol m^{-3} , based on the average difference between modeled and observed O_2 in the region. This correction is crucial for producing realistic benthic Fe fluxes under the anoxic conditions observed in the SBB, rather than fluxes at O_2 concentrations of 30 mmol m^{-3} .

Hypoxia off. The purpose of this experiment is to evaluate the importance of enhanced Fe fluxes under low- O_2 conditions in the SBB. Benthic Fe fluxes are calculated as in the high-flux experiment (Eq. 2), but they are capped at a constant value when O_2 decreases below a threshold of 65 mmol m^{-3} , which we chose as representative of hypoxic conditions (Deutsch et al., 2011). This change is applied only to the SBB and effectively bounds the benthic Fe release at $1.48 \mu\text{mol m}^{-2} \text{d}^{-1}$ when O_2 drops below the threshold for hypoxia.

Dust off. The purpose of this experiment is to evaluate the importance of aeolian Fe deposition in the CCS and to compare it with the benthic Fe fluxes. In this experiment, the atmospheric Fe deposition is set to zero; all other settings are identical to the high-flux experiment.

The baseline (high-flux) model simulation is run from 1995 to 2017. The other two model sensitivity experiments (hypoxia off and dust off) are branched off from the high-flux simulation in the year 2008 and run separately for 10 additional years (2008–2017). All model experiments use the same set of forcings and initial conditions. Results from the final 3 years (2015–2017) of the hypoxia-off and dust-off simulations are averaged and analyzed by comparing differences in biogeochemical fields (Fe, NO_3^- , and NPP) to the final 3 years of the high-flux run.

3 Results

3.1 In situ benthic Fe fluxes and model parameterization

Benthic Fe fluxes from in situ benthic chamber measurements during the AT42-19 expedition are shown in Table 1. High Fe flux was recorded at the anoxic depocenter stations (4.90 and $3.92 \text{ mmol m}^{-2} \text{d}^{-1}$ at SDRO and $3.49 \text{ mmol m}^{-2} \text{d}^{-1}$ at NDRO). Fe fluxes at the shallower hypoxic stations (NDT3C, NDT3B, and SDT3D) were an order of magnitude lower. The Fe flux at the hypoxic NDT3A station between NDRO and NDT3B was approximately half the flux observed at the depocenter.

Trends in the Fe fluxes suggest modulation by O_2 concentration, water depth, and/or bathymetry. We also note that the observed oxygen concentration represents a snapshot of bottom water conditions, while Fe fluxes likely reflect the oxygenation history at any given site. We observed a decrease in the Fe flux with a decrease in water depth (Fig. 2). There was also a slight trend of higher Fe fluxes with lower O_2 concentrations (most pronounced when O_2 reaches zero); however, since O_2 concentrations were relatively low at all stations ($< 10 \text{ mmol m}^{-3}$), it is difficult to distill a clear pattern based on the small dataset. Notably, the NDT3A station showed a high Fe flux despite exhibiting the same O_2 concentration as the shallower station SDT3D. Basin bathymetry may also contribute to observed differences in the flux. For instance, the deeper depocenter and A station showed higher averaged fluxes than the B, C, and D stations. We further noticed differences between the north and south extensions of the transect. The southern stations (SDRO and SDT3D) showed a higher Fe flux than the northern stations (NDRO and NDT3C).

We combined Fe fluxes determined during AT42-19 with previous estimates along the CCS, as compiled by Severmann et al. (2010), and analyzed them as a function of bottom water O_2 (Fig. 3). Pooled together, the measurements

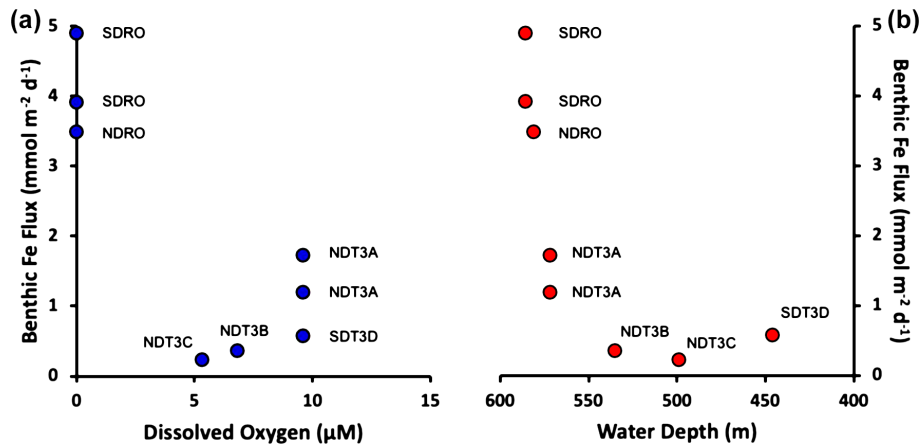


Figure 2. Benthic in situ Fe fluxes. (a) Fluxes as a function of O₂. (b) Fluxes as a function of (station) water depth. Note that water depth is shown from deep to shallow depths. See Table 1 for station details.

can be described reasonably well by an exponential increase in Fe fluxes with declining bottom water O₂ (Severmann et al., 2010), although significant variability around an exponential fit remains. This relationship is consistent with the Fe flux parameterization adopted in the ROMS-BEC model (Deutsch et al., 2021). Several observations from the AT42-19 cruise (red dots in Fig. 3) exceeded the range of previous measurements (blue dots in Fig. 3), likely owing to the anoxic or near-anoxic conditions in the water. Relative to the exponential fit to the dataset by Severmann et al. (2010) (yellow line in Fig. 3; see Eq. 2), the revised fit to the pooled data (purple line in Fig. 3; see Eq. 1) expands Fe fluxes by approximately a factor of 2 at O₂ concentrations close to zero but decreases the magnitude of the Fe fluxes at concentrations above approximately 130 mmol m⁻³.

3.2 Model evaluation: high-flux simulation

The high-flux simulation captures the magnitude and patterns of the observed dFe distribution in the upper ocean (Fig. 4), consistent with our knowledge of the ocean Fe cycle. In both the model and the observations, dFe concentrations are low at the surface, as a result of phytoplankton uptake, and increase gradually in subsurface waters due to organic matter remineralization in the water column and at the seafloor and benthic Fe fluxes from the sediment (Fig. S4). The highest dFe concentrations are found along the coast, likely related to high surface productivity and shallow carbon export and remineralization, combined with basin bathymetry and O₂ deficiency. In the open ocean, dFe concentrations are low in both the model and the observations, reflecting a combination of phytoplankton uptake, scavenging by sinking particles, and low external inputs.

Observational limitations prevent a more detailed validation of subsurface dFe patterns. Measurements of dFe concentrations in subsurface and deep waters (> 100 m) are currently very sparse in the CCS region and Southern Califor-

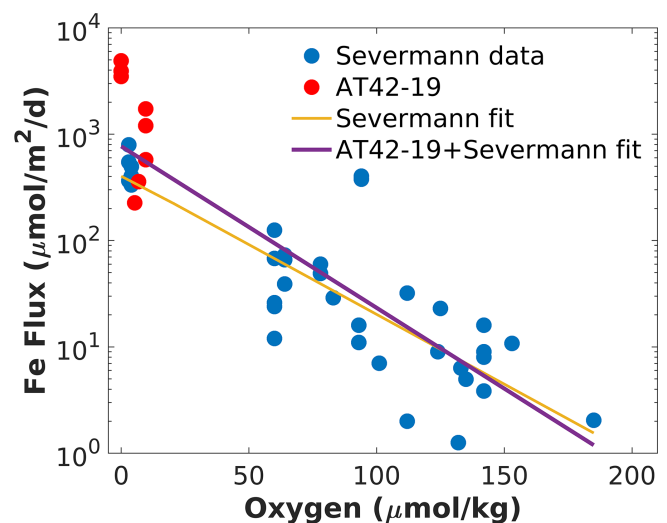


Figure 3. Combined benthic Fe flux data as a function of bottom oxygen. The blue dots show data from the compilation by Severmann et al. (2010), and the red dots show measurements from the AT42-19 cruise. The yellow line shows an exponential fit to the dataset by Severmann et al. (2010) (Eq. 2). The purple line shows an exponential fit to the combined dataset (Eq. 1). Note the logarithmic scale used for the y axis.

nia Borderland. Most of the dFe measurements for the SBB come from limited sampling conducted quarterly as part of selected California Cooperative Oceanic Fisheries Investigations (CalCOFI) cruises (King and Barbeau, 2011). These samples mostly focus on the mixed layer and are too sparse in space and time to capture the effects of deep-water renewal events that ventilate the anoxic basins and allow uplifting and transport of deep waters towards the surface.

The agreement of the model dFe with observations (correlation coefficient $R = 0.22$, $p < 0.01$) is similar to that of other ocean biogeochemical models (Tagliabue et al., 2016).

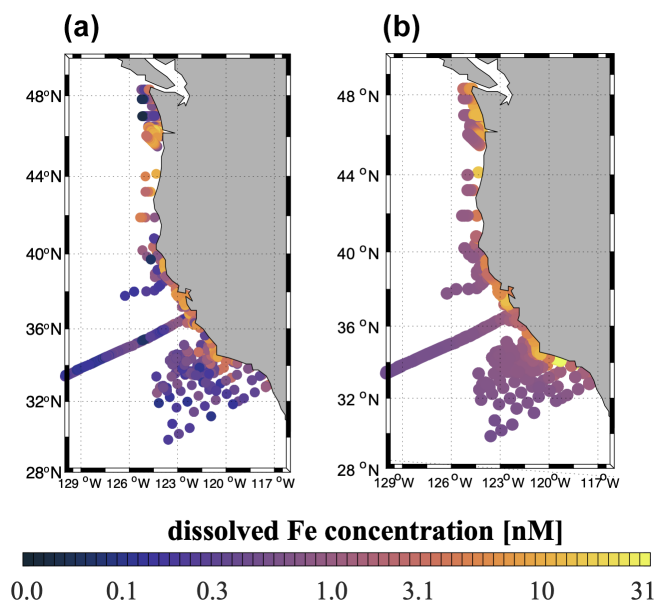


Figure 4. (a) Observed dFe concentrations (nM) from the US West Coast compilation (see Sect. 2.4) averaged between 0 and 100 m depth. (b) Annual mean modeled dFe concentrations (nM) averaged between 0 and 100 m depth, sampled at the same locations as the observations in (a).

The model tends to underestimate the sharp dFe gradient between coastal and open-ocean waters, overestimating dFe in the open ocean and producing too uniform concentrations offshore and at depth (Fig. 4). These biases are likely related to the simple Fe scavenging scheme, which assumes a constant Fe-binding ligand concentration of 0.6 nM. The small number and episodic nature of in situ measurements may also explain some of the mismatches between the model and observations.

At the scale of the CCS, the high-flux simulation produces lower surface dFe in the southern part of the domain (33 to 36° N) and higher surface concentration in the northern part (40 to 45° N) and near the central coast (Fig. 5a). While these patterns reflect a combination of internal Fe cycling and external inputs, the elevated dFe in the northern CCS, in particular offshore, can be partly attributed to higher aeolian deposition in that region (Fig. S5) as well as coastal inputs from the Juan De Fuca Strait (Deutsch et al., 2021).

The model reproduces the typical signature of coastal upwelling, with higher concentrations of NO_3^- nearshore in the central coast (36–40° N) and low concentrations in the Southern California Bight and offshore (Fig. 5b). Similarly, the model reproduces high values of NPP near the coast, in particular along the central coast, and rapidly decreasing values offshore (Fig. 5c). Relative to previous modeling work (Deutsch et al., 2021), our simulations generate somewhat lower surface NO_3^- concentrations close to the coast and sharper NPP gradients between the nearshore and offshore regions, which are consistent with the rapid decrease in pri-

mary productivity and chlorophyll shown by both satellite-based estimates and in situ data (Deutsch et al., 2021). These changes likely reflect the higher benthic Fe fluxes in our simulations (Eq. 1), which increase phytoplankton productivity and promote nutrient drawdown near the coast.

3.3 Hypoxia-off: impact of benthic Fe flux from low-oxygen bottom water

We quantify the importance of benthic Fe fluxes from low- O_2 bottom waters in the Southern California Borderland by analyzing results from the hypoxia-off experiment, in which we cap the high benthic Fe flux at a constant value ($1.48 \mu\text{mol m}^{-2} \text{d}^{-1}$) when O_2 declines below hypoxic conditions (65 mmol m^{-3} ; see Sect. 2.5) (Fig. 6). As expected, a decrease in benthic Fe flux from the anoxic basins in the hypoxia-off simulation leads to a decrease in the surface dFe concentration (Fig. 6a). This decrease is particularly significant along the coast of the SBB but also extends slightly into the open ocean (Fig. S6). This trend indicates that dFe released from low- O_2 sediment is effectively transported to the surface and offshore, where it can affect primary production. The decrease in surface dFe caused by reduced benthic release causes a decline in NPP near the coast (Fig. 6c), where phytoplankton rely the most on benthic-derived Fe. NPP also shows a patchy increase in some regions, especially between 32 and 33° N and between 34 and 35° N. This patchy increase can be explained by the relative importance of Fe vs. N limitation along a cross-shore productivity gradient. While phytoplankton is frequently Fe limited (up to 50 % of the time in the model) near the SBB coast, especially following upwelling events, it tends to be almost exclusively N limited moving offshore (Deutsch et al., 2021). This limitation pattern is consistent with observations from King and Barbeau (2011), who show that N : Fe ratios decrease moving from the coast to the open ocean (i.e., N is likely more limiting than Fe offshore). As Fe limitation reduces NPP near the coast in the hypoxia-off experiment, NO_3^- utilization also declines so that more NO_3^- can accumulate in surface waters (Fig. 6b). Shallow transport of excess NO_3^- in mesoscale eddies can further fertilize offshore waters (Damien et al., 2023), releasing local N limitation and fueling an increase in NPP (Fig. 6c).

3.4 Dust-off: role of atmospheric Fe deposition

We evaluate the importance of aeolian Fe sources in the dust-off simulation, in which atmospheric Fe deposition is set to zero. In this experiment, surface dFe decreases everywhere in the CCS, but the decrease is particularly evident in the open ocean and the northern part of the domain (Fig. 7a). This dFe decrease leads to a widespread reduction in NPP in the northern CCS (40 to 48° N, Fig. 7c), with stronger negative anomalies away from the coast. The decline in NPP is accompanied by a broad decrease in NO_3^- utilization, particularly evident offshore, where phytoplankton rely mostly on

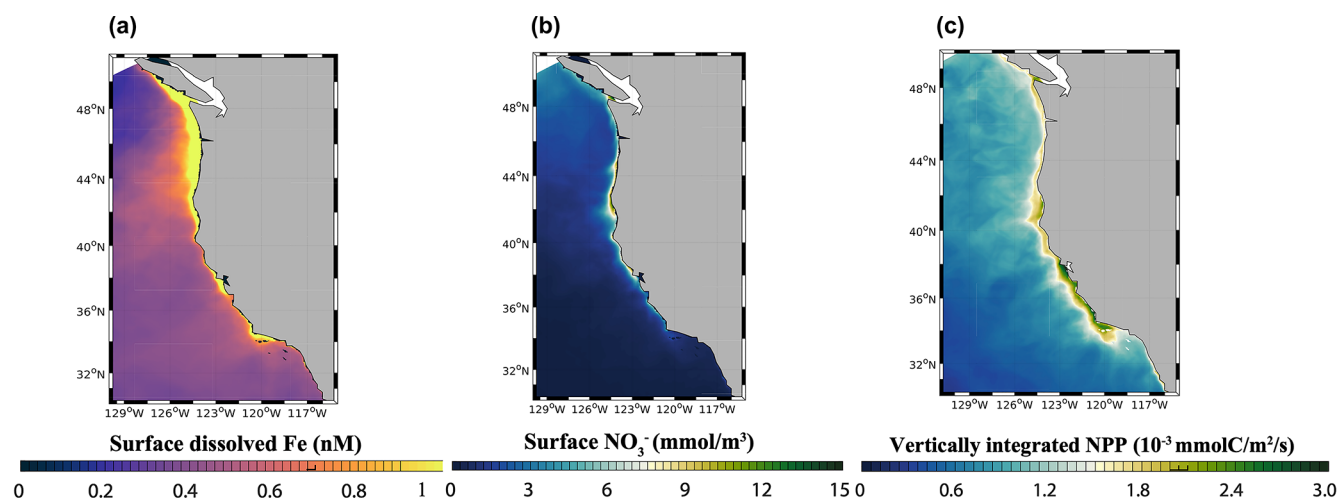


Figure 5. (a) Surface dFe concentration, (b) surface NO_3^- concentration, and (c) vertically integrated net primary production (NPP) from the high-flux model simulation.

Fe delivery by dust. In contrast, we observe a broad increase in NPP in the southern CCS (south of 40°S) and in coastal areas, likely reflecting increased availability of NO_3^- transported southward by the broad California Current. The response of NPP in coastal areas and the southern CCS, when the dust deposition of Fe is set to zero, demonstrates that phytoplankton in those regions relies mostly on benthic Fe fluxes, rather than on dust deposition, as the main source of Fe.

4 Discussion

4.1 Benthic Fe flux feedbacks on SBB biogeochemistry

The influence of bottom water O_2 concentration on the exchange of solutes between the sediment and the water column has been well documented (Soetaert et al., 2000; Sommer et al., 2016; Testa et al., 2013). Under hypoxic or anoxic bottom water conditions, organic matter sedimentation sustains anaerobic respiration at the sediment–water interface and in the sediment (Furrer and Wehrli, 1993; Middelburg and Levin, 2009). Reduced compounds accumulate in pore waters, forming chemical gradients (Widdows and Brinsley, 2002) that result in the flux of solutes such as Fe(II) out of the sediment and their accumulation in bottom water (Jørgensen and Nelson, 2004; McMahon and Chapelle, 1991; Middelburg and Levin, 2009; Yao et al., 2016). Similar conditions are observed in the SBB, where high sedimentation rates, water-column denitrification below the sill depth, and high pore-water concentrations of sulfide and Fe(II) have been observed (Behl and Kennett, 1996; Bray et al., 1999; Gericke et al., 2015; Sholkovitz and Soutar, 1975; Sigman et al., 2003; White et al., 2019).

The intense flux of dFe from the sediment suggests the potential for biogeochemical feedbacks in the SBB and more broadly in the CCS (as shown by Figs. 5–7). Under a positive feedback scenario (illustrated in Fig. 8a), anoxic and nearly anoxic bottom water conditions facilitate Fe(II) diffusion from the sediment into the bottom water. In the SBB, this Fe eventually reaches the surface via upwelling and mixing processes, which are likely enhanced in the presence of complex bathymetry and islands in the Southern California Bight (Kessouri et al., 2020). This additional dFe input fertilizes coastal waters and increases primary production. Newly formed organic matter eventually sinks towards the seafloor as a rain of organic particles, supporting low-oxygen concentrations in the bottom water and fueling anaerobic respiration, including Fe reduction, in the sediment. This chain of processes thus represents a positive feedback loop that maintains high Fe(II) release from the sediment, as long as the bottom water remains hypoxic or anoxic (Mills et al., 2004; Noffke et al., 2012; Sañudo-Wilhelmy et al., 2001; Dale et al., 2015; Wallmann et al., 2022).

Our simulations also indicate the potential for complex biogeochemical responses among Fe, NO_3^- , and NPP, which could limit the effects of these feedbacks. Specifically, the positive feedback loop is damped in our conceptual model by increased NO_3^- limitation and elevated N loss in anoxic sediments under oxygen-deficient bottom waters at higher Fe supply (illustrated by Fig. 8b), which would in turn limit the increase in NPP. Transport of N-depleted coastal waters can further reduce NPP offshore, counteracting the positive feedback. In addition, the positive feedback would also be damped by Fe scavenging, which is magnified at high dissolved Fe concentrations, unless Fe-binding ligands also increase. This damping effect is particularly strong in our model, where a constant ligand concentration of 0.6 nM is used, above which scavenging rapidly increases (Sect. 2).

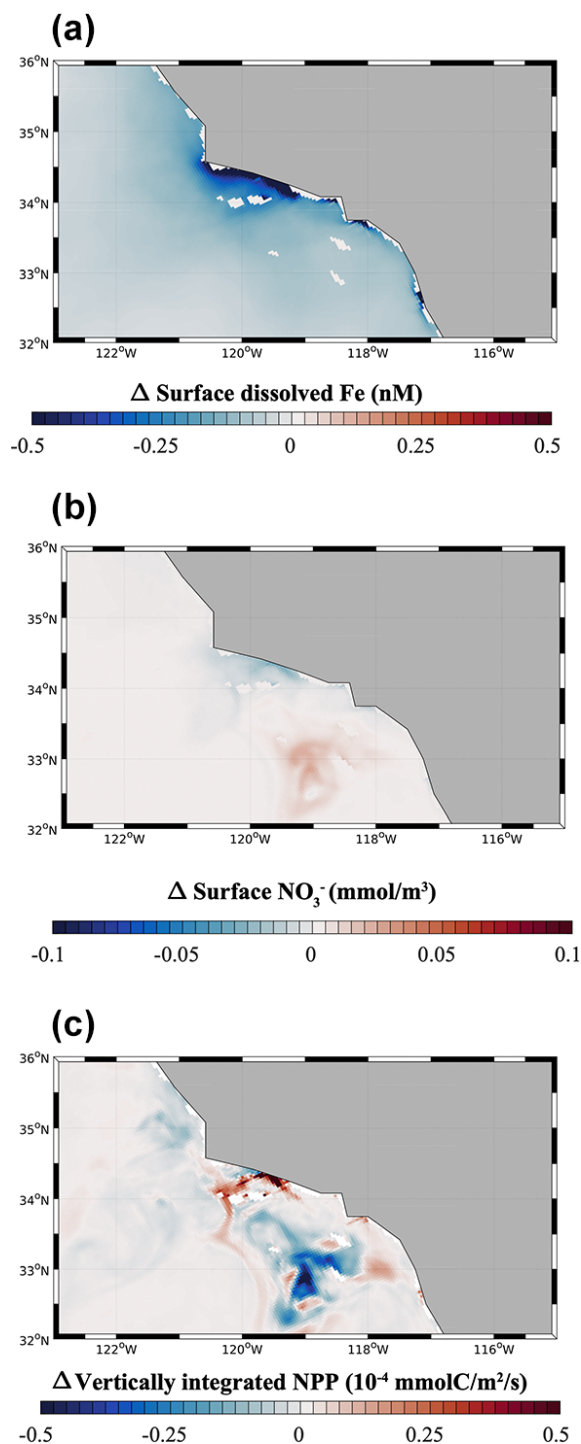


Figure 6. (a) Surface dFe anomalies, (b) Surface NO₃⁻ anomalies, and (c) vertically integrated net primary production (NPP) from the hypoxia-off model run relative to the high-flux model run. The maps focus on the region around the SBB.

Such a negative feedback between scavenging and benthic Fe fluxes is consistent with the global modeling study by Somes et al. (2021).

Additional processes may further modulate these feedback loops. Increased anoxia in bottom water and sediment favors the removal of fixed N by denitrification (Goericke et al., 2015; White et al., 2019). Upwelling of NO₃⁻-depleted waters would then reduce surface productivity by increasing N limitation (Gruber and Deutsch, 2014). Release of Fe(II) from the sediment could also impact phosphate dynamics. Phosphate is scavenged by Fe during oxidation of Fe(II) in the water column and sediment because of the ability of Fe(III) minerals to bind it. After burial, phosphate is released due to reduction in solid Fe(III) minerals to dissolved Fe(II) and diffuses upward to be either re-adsorbed by Fe(III) at the oxic sediment–water interface or released to the bottom water under anoxic conditions (Dijkstra et al., 2014). The latter scenario is consistent with our in situ benthic flux chamber measurements, revealing increased phosphate release from the sediment with increased depth in the SBB (Yousavich et al., 2024). Higher release of phosphate into the water column, and transport to the surface, could decrease the N : P ratio of phytoplankton, especially downstream of waters where denitrification occurred (Deutsch et al., 2007). In the presence of N limitation, these conditions could favor the activity of nitrogen-fixing microorganisms (Mills et al., 2004; Noffke et al., 2012; Sañudo-Wilhelmy et al., 2001), which could further modulate surface NPP (Deutsch et al., 2007).

4.2 Contribution of physical transport to surface Fe

Our numerical experiments suggest that Fe released into the deep SBB can reach surface waters and fertilize them. This finding highlights the critical role of bottom water upwelling and mixing in the deep basins of the Southern California Borderland. There is ample literature describing seasonal surface circulation and bottom water renewal and their effect on nutrients in the SBB (Bray et al., 1999; Hendershott and Winant, 1996; Sholkovitz and Gieskes, 1971). However, the frequency and rate of seasonal bottom water flushing events and the processes responsible for vertical mixing and upwelling across hundreds of meters remain poorly understood (Shiller et al., 1985; Sholkovitz and Gieskes, 1971; White et al., 2019). It is likely that interaction between wind-driven upwelling events and submesoscale eddies, which are particularly intense inside the Santa Barbara Channel (Kessouri et al., 2020), favors upward mixing of deep bottom water in the wake of flushing events, connecting deep bottom waters to the surface.

4.3 Quantifying expansion of anoxia in the SBB

Changes in source waters and global O₂ loss have contributed to decreasing O₂ levels throughout the Southern California Bight and the SBB (Zhou et al., 2022). With the outlook

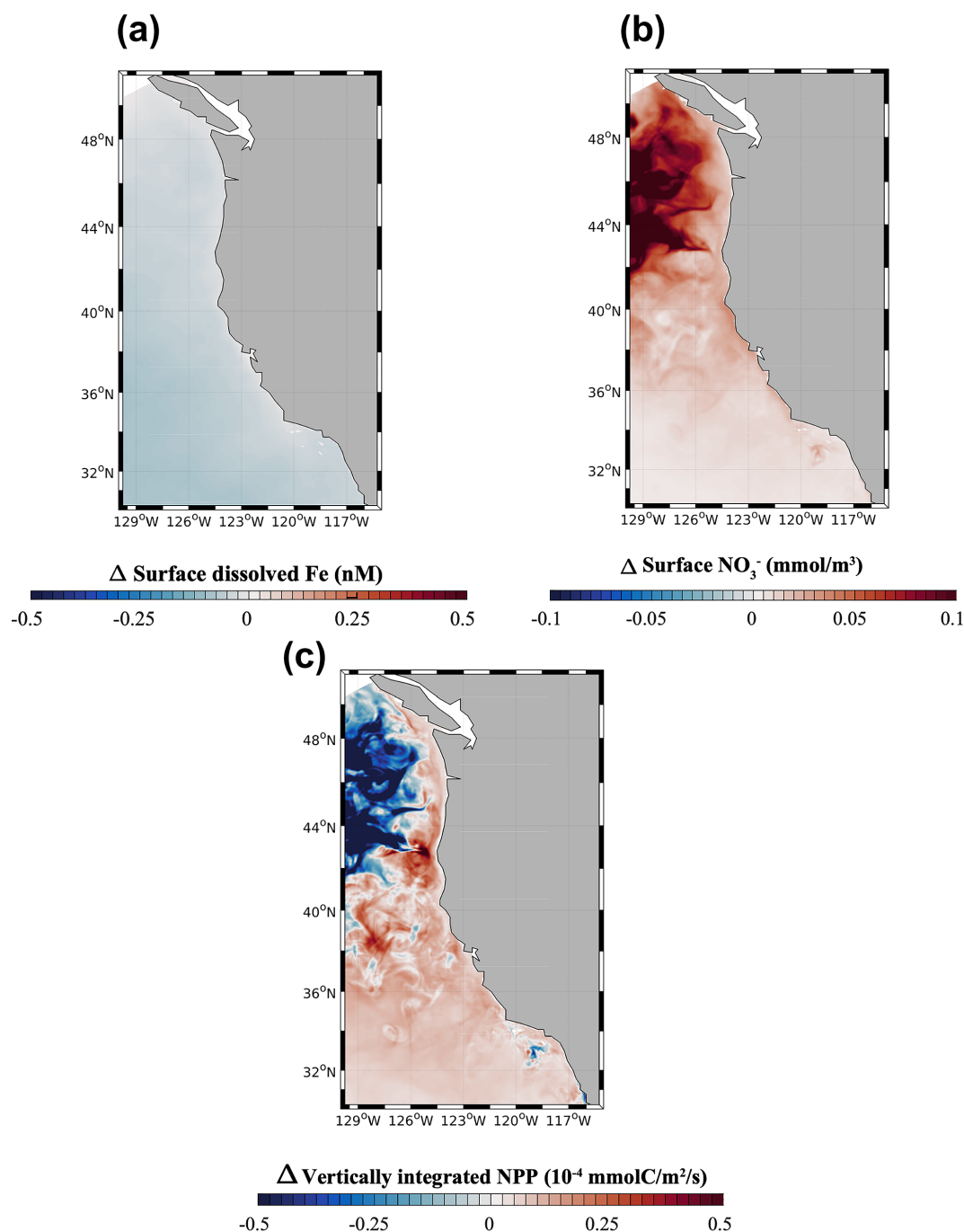


Figure 7. (a) Surface dissolved Fe, (b) surface NO_3^- anomalies, and (c) vertically integrated net primary production (NPP) from the dust-off model run relative to the high-flux model run.

of a continuing decline in oceanic O_2 (Bopp et al., 2013; Kwiatkowski et al., 2020), quantifying the expansion of hypoxic and anoxic zones in the SBB is vital to understand the dynamics and fate of Fe(II) and other reduced compounds, such as ammonium and hydrogen sulfide, in deep low-oxygen waters. In the SBB, bottom water renewal events have experienced a decline in frequency and magnitude, driv-

ing an expansion of hypoxic and anoxic conditions in deep waters (White et al., 2019). This expansion has led to an increase in anaerobic reactions, such as denitrification in the water column (White et al., 2019) and sulfur cycling in the sediment (Valentine et al., 2016). Expansion of low- O_2 waters could intensify the positive feedback loop among Fe release, NPP, and O_2 loss (Fig. 8). However, to date, despite

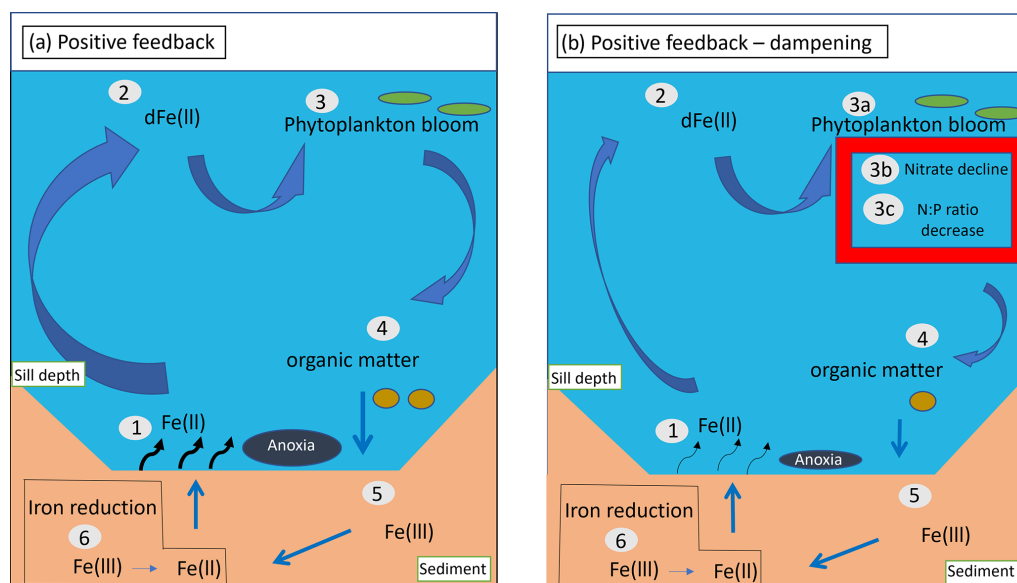


Figure 8. Schematic illustrating feedback loops among benthic Fe release, nutrient cycles, and productivity in the Santa Barbara Basin. **(a)** Positive feedback loop: (1) benthic Fe is released into the oxygen-poor bottom water, (2) upwelled Fe reaches the surface ocean, increasing dissolved Fe concentrations, (3) dissolved Fe is assimilated by phytoplankton, fueling blooms and production of organic matter and siderophores, i.e., ligands used to chelate ferric iron, (4) organic matter is exported from the surface to the deep ocean, (5) organic matter accumulates at the sediment–water interface, and (6) during remineralization, iron-reducing bacteria reduce Fe(III) to Fe(II), increasing benthic dFe release. **(b)** Positive feedback loop – dampening: (1)–(3) (not including 3b and 3c) and (4)–(6) are identical to **(a)**. Parts (3b) and (3c) illustrate the decline of NO_3^- at the surface caused by the reduction in Fe limitation, which together with increased denitrification in anoxic waters and sediment would limit the potential increase in primary production and export from the surface caused by Fe fertilization. Together with enhanced release of phosphate from anoxic sediment, a reduction in the available NO_3^- could also reduce the N:P ratio of phytoplankton. Ultimately, the effect of a decrease in NO_3^- on export and remineralization of organic matter would limit the increase in benthic Fe(II) fluxes, dampening the positive feedback.

growing evidence of more frequent anoxia, there is no clear quantitative record of the vertical or horizontal expansions of oxygen-deficient waters in the SBB.

5 Conclusion

Our field campaign in the SBB measured a remarkably high flux of Fe(II) from the sediment ($0.23\text{--}4.9\text{ mmol m}^{-2}\text{ d}^{-1}$), greater than in previous studies from this region (Severmann et al., 2010) and from other oxygen minimum zones (Dale et al., 2015; Homoky et al., 2021). While these observations are based on snapshots of O_2 and Fe fluxes, they have implications for the temporal variability of Fe supply. High benthic Fe fluxes are observed during the anoxic fall season, while seasonal flushing in winter and spring likely decreases them by increasing bottom water O_2 and Fe oxidation and retention near the sediment.

Using a series of simulations with an ocean biogeochemical model, we show that this high Fe release from deep, low-oxygen sediment can reach the surface and impact nutrients and productivity in the SBB and the Southern California Bight, where Fe is often limiting (Hogle et al., 2018). We also highlight the impacts of coastal Fe inputs on waters fur-

ther offshore. While phytoplankton in coastal areas directly benefits from Fe fertilization, increased NO_3^- utilization in coastal waters can increase N limitation of phytoplankton further downstream in open-ocean areas. Thus, benthic Fe fluxes can modulate Fe and NO_3^- limitation in ways that partially counteract one another along the cross-shore productivity gradient of the CCS. Our simulations also suggest that Fe inputs from atmospheric deposition are mostly important in the open ocean north of 40°N , where phytoplankton rely on Fe delivery by dust. However, we also show that changes in atmospheric Fe deposition can affect ocean productivity in the southern CCS by altering NO_3^- utilization further downstream. Our results support the idea that benthic Fe fluxes are the major source of Fe in the southern CCS and are supplemented by atmospheric deposition in northwestern and offshore waters, leading to relatively high NPP coastwide.

We suggest that benthic Fe fluxes from deep anoxic basins reach the surface in the SBB, contributing to feedbacks between Fe and NO_3^- limitation and NPP. Specifically, high Fe fluxes from low-oxygen sediment support higher NPP near the coast, in turn leading to increased respiration and O_2 loss at depth, maintaining high Fe release. This positive feedback is damped by increased NO_3^- limitation, which reduces NPP

downstream of coastal regions. This benthic–pelagic coupling demonstrates the importance of sediment-derived Fe fluxes on the coastal ecosystem of the CCS and the role of vertical transport processes in connecting deep environments to surface waters along continental margins. Our results are thus consistent with previous work from the Peruvian coastal upwelling (Wallmann et al., 2022), suggesting that oceanic O₂ loss could drive an increase in benthic Fe fluxes, enhancing local productivity and leading to further O₂ loss. This positive feedback could be stabilized by loss of fixed nitrogen under expanded anaerobic conditions.

It is likely that feedbacks of the type highlighted by Wallmann et al. (2022) and our work in the SBB are at play more broadly along low-oxygen upwelling systems and coastal oxygen minimum zones. Further studies should focus on the coupling between benthic processes and Fe and nutrient cycling in these regions. For example, fixed nitrogen loss by denitrification and enhanced release of phosphorous under low-oxygen bottom water are likely to further modulate these interactions. Seasonal studies based on stable isotope, radio-tracer, and geochemical techniques are required to track the fate and transport of nutrients in low-O₂ coastal regions, clarifying the dynamics and sensitivities of the underlying microbial metabolisms. Ocean biogeochemical models for regional and global studies should incorporate new observations of benthic fluxes and their sensitivity to bottom O₂ and other environmental variables. This would expand the ability of models to better capture the effects of long-term oceanic O₂ loss and the feedbacks between benthic nutrient fluxes and surface productivity.

Code availability. The physical and biogeochemical codes used for our simulations as well as the model output can be accessed at <https://doi.org/10.5281/zenodo.10247145> (Robinson and Pham, 2023).

Data availability. In situ benthic Fe flux data are accessible through the Biological & Chemical Oceanography Data Management Office (BCO-DMO) under the following: <https://doi.org/10.26008/1912/bco-dmo.896706.1> (Treude and Valentine, 2023).

Supplement. The supplement related to this article is available online at: <https://doi.org/10.5194/bg-21-773-2024-supplement>.

Author contributions. DR, TT, DB, and ALDP conceived this study. DR, DJY, FJ, FW, ECA, KMG, DLV, and TT conducted the sampling at sea. DJY transformed and interpreted ROV *Jason* data. FJ and FW deployed and maintained benthic flux chambers. DYJ and DR analyzed Fe(II) and assisted with the flux calculation. MM provided the compiled Fe measurements along the US West Coast. ALDP and MSB performed the model simulations. DR, DB, ALDP, and TT wrote the paper with input from all co-authors.

Competing interests. At least one of the (co-)authors is a member of the editorial board of *Biogeosciences*. The peer-review process was guided by an independent editor, and the authors also have no other competing interests to declare.

Disclaimer. Publisher’s note: Copernicus Publications remains neutral with regard to jurisdictional claims made in the text, published maps, institutional affiliations, or any other geographical representation in this paper. While Copernicus Publications makes every effort to include appropriate place names, the final responsibility lies with the authors.

Special issue statement. This article is part of the special issue “Low-oxygen environments and deoxygenation in open and coastal marine waters”. It is not associated with a conference.

Acknowledgements. We thank the captain and crew of R/V *Atlantis*, the crew of ROV *Jason*, the crew of AUV *Sentry*, and the science party of research cruise AT42-19 for their technical and logistical support. We thank Qianhui Qin, Molly O’Beirne, Aran Mazariegos, Xiadani Moreno, and Alec Eastman for assisting with shipboard analyses.

Financial support. This research has been supported by the National Science Foundation (grant nos. OCE-1829981, OCE-182998, OCE-1756947, OCE-1830033, OCE-2023493, and 1548562) and the San Diego Supercomputer Center (grant no. TG-OCE170017).

Review statement. This paper was edited by Caroline P. Slomp and reviewed by Christopher Somes and one anonymous referee.

References

- Aumont, O., Ethé, C., Tagliabue, A., Bopp, L., and Gehlen, M.: PISCES-v2: an ocean biogeochemical model for carbon and ecosystem studies, *Geosci. Model Dev.*, 8, 2465–2513, <https://doi.org/10.5194/gmd-8-2465-2015>, 2015.
- Behl, R. J. and Kennett, J. P.: Brief interstadial events in the Santa Barbara basin, NE Pacific, during the past 60 kyr, *Nature*, 379, 243–246, <https://doi.org/10.1038/379243a0>, 1996.
- Biller, D. V. and Bruland, K. W.: Sources and distributions of Mn, Fe, Co, Ni, Cu, Zn, and Cd relative to macronutrients along the central California coast during the spring and summer upwelling season, *Mar. Chem.*, 155, 50–70, <https://doi.org/10.1016/j.marchem.2013.06.003>, 2013.
- Boiteau, R. M., Till, C. P., Coale, T. H., Fitzsimmons, J. N., Bruland, K. W., and Repeta, D. J.: Patterns of iron and siderophore distributions across the California Current System, *Limnol. Oceanogr.*, 64, 376–389, <https://doi.org/10.1002/lno.11046>, 2019.
- Bopp, L., Resplandy, L., Orr, J. C., Doney, S. C., Dunne, J. P., Gehlen, M., Halloran, P., Heinze, C., Ilyina, T., Séférian, R.,

- Tjiputra, J., and Vichi, M.: Multiple stressors of ocean ecosystems in the 21st century: projections with CMIP5 models, *Biogeosciences*, 10, 6225–6245, <https://doi.org/10.5194/bg-10-6225-2013>, 2013.
- Brander, K., Cochrane, K., Barange, M., and Soto, D.: Climate Change Implications for Fisheries and Aquaculture, in: *Climate Change Impacts on Fisheries and Aquaculture*, edited by: Phillips, B. F. and Pérez-Ramírez, M., John Wiley & Sons, Ltd, Chichester, UK, 45–62, <https://doi.org/10.1002/9781119154051.ch3>, 2017.
- Bray, N. A., Keyes, A., and Morawitz, W. M. L.: The California Current system in the Southern California Bight and the Santa Barbara Channel, *J. Geophys. Res.-Oceans*, 104, 7695–7714, <https://doi.org/10.1029/1998JC900038>, 1999.
- Bruland, K. W., Rue, E. L., and Smith, G. J.: Iron and macronutrients in California coastal upwelling regimes: Implications for diatom blooms, *Limnol. Oceanogr.*, 46, 1661–1674, <https://doi.org/10.4319/lo.2001.46.7.1661>, 2001.
- Bruland, K. W., Middag, R., and Lohan, M. C.: Controls of Trace Metals in Seawater, in: *Treatise on Geochemistry*, edited by: Holland, H. D. Turekian, K. K., Elsevier, 19–51, <https://doi.org/10.1016/B978-0-08-095975-7.00602-1>, 2014.
- Bundy, R. M., Biller, D. V., Buck, K. N., Bruland, K. W., and Barbeau, K. A.: Distinct pools of dissolved iron-binding ligands in the surface and benthic boundary layer of the California Current, *Limnol. Oceanogr.*, 59, 769–787, <https://doi.org/10.4319/lo.2014.59.3.0769>, 2014.
- Bundy, R. M., Abdulla, H. A. N., Hatcher, P. G., Biller, D. V., Buck, K. N., and Barbeau, K. A.: Iron-binding ligands and humic substances in the San Francisco Bay estuary and estuarine-influenced shelf regions of coastal California, *Mar. Chem.*, 173, 183–194, <https://doi.org/10.1016/j.marchem.2014.11.005>, 2015.
- Bundy, R. M., Jiang, M., Carter, M., and Barbeau, K. A.: Iron-Binding Ligands in the Southern California Current System: Mechanistic Studies, *Front. Mar. Sci.*, 3, 27, <https://doi.org/10.3389/fmars.2016.00027>, 2016.
- Capet, X., Campos, E. J., and Paiva, A. M.: Submesoscale activity over the Argentinian shelf, *Geophys. Res. Lett.*, 35, L15605, <https://doi.org/10.1029/2008GL034736>, 2008.
- Carr, M.-E. and Kearns, E. J.: Production regimes in four Eastern Boundary Current systems, *Deep-Sea Res. Pt. II*, 50, 3199–3221, <https://doi.org/10.1016/j.dsr2.2003.07.015>, 2003.
- Chappell, P., Armbrust, E., Barbeau, K., Bundy, R., Moffett, J., Vedamati, J., and Jenkins, B.: Patterns of diatom diversity correlate with dissolved trace metal concentrations and longitudinal position in the northeast Pacific coastal-offshore transition zone, *Mar. Ecol.-Prog. Ser.*, 609, 69–86, <https://doi.org/10.3354/meps12810>, 2019.
- Chase, Z.: Iron, nutrient, and phytoplankton distributions in Oregon coastal waters, *J. Geophys. Res.*, 107, 3174, <https://doi.org/10.1029/2001JC000987>, 2002.
- Chase, Z., Johnson, K. S., Elrod, V. A., Plant, J. N., Fitzwater, S. E., Pickell, L., and Sakamoto, C. M.: Manganese and iron distributions off central California influenced by upwelling and shelf width, *Mar. Chem.*, 95, 235–254, <https://doi.org/10.1016/j.marchem.2004.09.006>, 2005.
- Chavez, F. P. and Messié, M.: A comparison of Eastern Boundary Upwelling Ecosystems, *Prog. Oceanogr.*, 83, 80–96, <https://doi.org/10.1016/j.pocean.2009.07.032>, 2009.
- Dale, A. W., Nickelsen, L., Scholz, F., Hensen, C., Oschlies, A., and Wallmann, K.: A revised global estimate of dissolved iron fluxes from marine sediments: GLOBAL BENTHIC IRON FLUXES, *Global Biogeochem. Cy.*, 29, 691–707, <https://doi.org/10.1002/2014GB005017>, 2015.
- Damien, P., Bianchi, D., McWilliams, J. C., Kessouri, F., Deutsch, C., Chen, R., and Renault, L.: Enhanced Biogeochemical Cycling Along the U.S. West Coast Shelf, *Global Biogeochem. Cy.*, 37, e2022GB007572, <https://doi.org/10.1029/2022GB007572>, 2023.
- Deutsch, C., Sarmiento, J. L., Sigman, D. M., Gruber, N., and Dunne, J. P.: Spatial coupling of nitrogen inputs and losses in the ocean, *Nature*, 445, 163–167, <https://doi.org/10.1038/nature05392>, 2007.
- Deutsch, C., Brix, H., Ito, T., Frenzel, H., and Thompson, L.: Climate-Forced Variability of Ocean Hypoxia, *Science*, 333, 336–339, <https://doi.org/10.1126/science.1202422>, 2011.
- Deutsch, C., Frenzel, H., McWilliams, J. C., Renault, L., Kessouri, F., Howard, E., Liang, J.-H., Bianchi, D., and Yang, S.: Biogeochemical variability in the California Current System, *Prog. Oceanogr.*, 196, 102565, <https://doi.org/10.1016/j.pocean.2021.102565>, 2021.
- Dijkstra, N., Kraal, P., Kuypers, M. M. M., Schnetger, B., and Slomp, C. P.: Are Iron-Phosphate Minerals a Sink for Phosphorus in Anoxic Black Sea Sediments?, *PLOS ONE*, 9, e101139, <https://doi.org/10.1371/journal.pone.0101139>, 2014.
- Evans, N., Schroeder, I. D., Pozo Buil, M., Jacox, M. G., and Bograd, S. J.: Drivers of Subsurface Deoxygenation in the Southern California Current System, *Geophys. Res. Lett.*, 47, e2020GL089274, <https://doi.org/10.1029/2020GL089274>, 2020.
- Firme, G. F., Rue, E. L., Weeks, D. A., Bruland, K. W., and Hutchins, D. A.: Spatial and temporal variability in phytoplankton iron limitation along the California coast and consequences for Si, N, and C biogeochemistry: SPATIAL AND TEMPORAL VARIABILITY IN PHYTOPLANKTON IRON, *Global Biogeochem. Cy.*, 17, 1016, <https://doi.org/10.1029/2001GB001824>, 2003.
- Furrer, G. and Wehrli, B.: Biogeochemical processes at the sediment-water interface: measurements and modeling, *Appl. Geochem.*, 8, 117–119, [https://doi.org/10.1016/S0883-2927\(09\)80021-8](https://doi.org/10.1016/S0883-2927(09)80021-8), 1993.
- García-Reyes, M. and Largier, J.: Observations of increased wind-driven coastal upwelling off central California, *J. Geophys. Res.*, 115, C04011, <https://doi.org/10.1029/2009JC005576>, 2010.
- Goericke, R., Bograd, S. J., and Grundle, D. S.: Denitrification and flushing of the Santa Barbara Basin bottom waters, *Deep-Sea Res. Pt. II*, 112, 53–60, <https://doi.org/10.1016/j.dsr2.2014.07.012>, 2015.
- Grasshoff, K., Ehrhardt, M., and Kremling, K.: *Methods of seawater analysis*, Wiley-VCH Verlag GmbH, Weinheim, 632 pp., ISBN 3-527-29589-5, 1999.
- Gruber, N. and Deutsch, C.: Redfield’s evolving legacy, *Nat. Geosci.*, 7, 853–855, <https://doi.org/10.1038/ngeo2308>, 2014.
- Hawco, N. J., Barone, B., Church, M. J., Babcock-Adams, L., Repeta, D. J., Wear, E. K., Foreman, R. K., Björkman, K. M., Bent, S., Van Mooy, B. A. S., Sheyn, U., DeLong, E. F., Acker, M., Kelly, R. L., Nelson, A., Ranieri, J., Clemente, T. M., Karl, D. M., and John, S. G.: Iron Depletion in the Deep Chlorophyll Maximum: Mesoscale Eddies as Natural Iron Fertilization

- Experiments, *Global Biogeochem. Cy.*, 35, e2021GB007112, <https://doi.org/10.1029/2021GB007112>, 2021.
- Hendershott, M. C. and Winant, C. D.: Surface circulation in the Santa Barbara channel, *Oceanography*, 9, 114–121, 1996.
- Hogle, S. L., Dupont, C. L., Hopkinson, B. M., King, A. L., Buck, K. N., Roe, K. L., Stuart, R. K., Allen, A. E., Mann, E. L., Johnson, Z. I., and Barbeau, K. A.: Pervasive iron limitation at subsurface chlorophyll maxima of the California Current, *P. Natl. Acad. Sci. USA*, 115, 13300–13305, <https://doi.org/10.1073/pnas.1813192115>, 2018.
- Homoky, W. B., Conway, T. M., John, S. G., König, D., Deng, F., Tagliabue, A., and Mills, R. A.: Iron colloids dominate sedimentary supply to the ocean interior, *P. Natl. Acad. Sci. USA*, 118, e2016078118, <https://doi.org/10.1073/pnas.2016078118>, 2021.
- John, S. G., Mendez, J., Moffett, J., and Adkins, J.: The flux of iron and iron isotopes from San Pedro Basin sediments, *Geochim. Cosmochim. Ac.*, 93, 14–29, <https://doi.org/10.1016/j.gca.2012.06.003>, 2012.
- Johnson, K. S., Elrod, V. A., Fitzwater, S. E., Plant, J. N., Chavez, F. P., Tanner, S. J., Gordon, R. M., Westphal, D. L., Perry, K. D., Wu, J., and Karl, D. M.: Surface ocean-lower atmosphere interactions in the Northeast Pacific Ocean Gyre: Aerosols, iron, and the ecosystem response, *Global Biogeochem. Cy.*, 17, 1063, <https://doi.org/10.1029/2002GB002004>, 2003.
- Jørgensen, B. B. and Nelson, D. C.: Sulfide oxidation in marine sediments: Geochemistry meets microbiology, in: *Sulfur Biogeochemistry – Past and Present*, GSA Special Papers, <https://doi.org/10.1130/0-8137-2379-5.63>, 2004.
- Kessouri, F., Bianchi, D., Renault, L., McWilliams, J. C., Frenzel, H., and Deutsch, C. A.: Submesoscale Currents Modulate the Seasonal Cycle of Nutrients and Productivity in the California Current System, *Global Biogeochem. Cy.*, 34, e2020GB006578, <https://doi.org/10.1029/2020GB006578>, 2020.
- King, A. L. and Barbeau, K. A.: Dissolved iron and macronutrient distributions in the southern California Current System, *J. Geophys. Res.*, 116, C03018, <https://doi.org/10.1029/2010JC006324>, 2011.
- Kononets, M., Tengberg, A., Nilsson, M., Ekeröth, N., Hylén, A., Robertson, E. K., van de Velde, S., Bonaglia, S., Rütting, T., Blomqvist, S., and Hall, P. O. J.: In situ incubations with the Gothenburg benthic chamber landers: Applications and quality control, *J. Marine Syst.*, 214, 103475, <https://doi.org/10.1016/j.jmarsys.2020.103475>, 2021.
- Kwiatkowski, L., Torres, O., Bopp, L., Aumont, O., Chamberlain, M., Christian, J. R., Dunne, J. P., Gehlen, M., Ilyina, T., John, J. G., Lenton, A., Li, H., Lovenduski, N. S., Orr, J. C., Palmieri, J., Santana-Falcón, Y., Schwinger, J., Séférian, R., Stock, C. A., Tagliabue, A., Takano, Y., Tjiputra, J., Toyama, K., Tsujino, H., Watanabe, M., Yamamoto, A., Yool, A., and Ziehn, T.: Twenty-first century ocean warming, acidification, deoxygenation, and upper-ocean nutrient and primary production decline from CMIP6 model projections, *Biogeosciences*, 17, 3439–3470, <https://doi.org/10.5194/bg-17-3439-2020>, 2020.
- Mahowald, N. M., Muhs, D. R., Levis, S., Rasch, P. J., Yoshioka, M., Zender, C. S., and Luo, C.: Change in atmospheric mineral aerosols in response to climate: Last glacial period, preindustrial, modern, and doubled carbon dioxide climates: DUST RESPONSE TO CLIMATE, *J. Geophys. Res.-Atmos.*, 111, D10202, <https://doi.org/10.1029/2005JD006653>, 2006.
- McMahon, P. B. and Chapelle, F. H.: Microbial production of organic acids in aquitard sediments and its role in aquifer geochemistry, *Nature*, 349, 233–235, <https://doi.org/10.1038/349233a0>, 1991.
- Middelburg, J. J. and Levin, L. A.: Coastal hypoxia and sediment biogeochemistry, *Biogeosciences*, 6, 1273–1293, <https://doi.org/10.5194/bg-6-1273-2009>, 2009.
- Mills, M. M., Ridame, C., Davey, M., La Roche, J., and Geider, R. J.: Iron and phosphorus co-limit nitrogen fixation in the eastern tropical North Atlantic, *Nature*, 429, 292–294, <https://doi.org/10.1038/nature02550>, 2004.
- Moore, J. K. and Braucher, O.: Sedimentary and mineral dust sources of dissolved iron to the world ocean, *Biogeosciences*, 5, 631–656, <https://doi.org/10.5194/bg-5-631-2008>, 2008.
- Moore, J. K., Doney, S. C., Kleypas, J. A., Glover, D. M., and Fung, I. Y.: An intermediate complexity marine ecosystem model for the global domain, *Deep-Sea Res. Pt. II*, 49, 403–462, [https://doi.org/10.1016/S0967-0645\(01\)00108-4](https://doi.org/10.1016/S0967-0645(01)00108-4), 2001.
- Moore, J. K., Doney, S. C., and Lindsay, K.: Upper ocean ecosystem dynamics and iron cycling in a global three-dimensional model: GLOBAL ECOSYSTEM-BIOGEOCHEMICAL MODEL, *Global Biogeochem. Cy.*, 18, GB4028, <https://doi.org/10.1029/2004GB002220>, 2004.
- Noffke, A., Hensen, C., Sommer, S., Scholz, F., Bohlen, L., Mosch, T., Graco, M., and Wallmann, K.: Benthic iron and phosphorus fluxes across the Peruvian oxygen minimum zone, *Limnol. Oceanogr.*, 57, 851–867, <https://doi.org/10.4319/lo.2012.57.3.0851>, 2012.
- Pham, A. L. D. and Ito, T.: Formation and Maintenance of the GEOTRACES Subsurface-Dissolved Iron Maxima in an Ocean Biogeochemistry Model, *Global Biogeochem. Cy.*, 32, 932–953, <https://doi.org/10.1029/2017GB005852>, 2018.
- Pham, A. L. D. and Ito, T.: Ligand Binding Strength Explains the Distribution of Iron in the North Atlantic Ocean, *Geophys. Res. Lett.*, 46, 7500–7508, <https://doi.org/10.1029/2019GL083319>, 2019.
- Pozo Buil, M. and Di Lorenzo, E.: Decadal dynamics and predictability of oxygen and subsurface tracers in the California Current System, *Geophys. Res. Lett.*, 44, 4204–4213, <https://doi.org/10.1002/2017GL072931>, 2017.
- Qin, Q., Kinnaman, F. S., Gosselin, K. M., Liu, N., Treude, T., and Valentine, D. L.: Seasonality of water column methane oxidation and deoxygenation in a dynamic marine environment, *Geochim. Cosmochim. Ac.*, 336, 219–230, <https://doi.org/10.1016/j.gca.2022.09.017>, 2022.
- Reimers, C. E., Lange, C. B., Tabak, M., and Bernhard, J. M.: Seasonal spillover and varve formation in the Santa Barbara Basin, California, *Limnol. Oceanogr.*, 35, 1577–1585, <https://doi.org/10.4319/lo.1990.35.7.1577>, 1990.
- Renault, L., Deutsch, C., McWilliams, J. C., Frenzel, H., Liang, J.-H., and Colas, F.: Partial decoupling of primary productivity from upwelling in the California Current system, *Nat. Geosci.*, 9, 505–508, <https://doi.org/10.1038/ngeo2722>, 2016.
- Renault, L., McWilliams, J. C., Kessouri, F., Jousse, A., Frenzel, H., Chen, R., and Deutsch, C.: Evaluation of high-resolution atmospheric and oceanic simulations of the California Current System, *Prog. Oceanogr.*, 195, 102564, <https://doi.org/10.1016/j.pocean.2021.102564>, 2021.

- Robinson, D. and Pham, A.: V2: Model outputs and scripts to produce figures in manuscript “Iron ”Ore” Nothing: Benthic iron fluxes from the oxygen-deficient Santa Barbara Basin enhance phytoplankton productivity in surface water”, Zenodo [code], <https://doi.org/10.5281/zenodo.10247145>, 2023.
- Sañudo-Wilhelmy, S., Kustka, A., Gobler, C., Hutchins, D., Yang, M., Lwiza, K., Burns, J., Raven, J., and Carpenter, E.: Phosphorus limitation of nitrogen fixation by Trichodesmium in the central Atlantic Ocean, *Nature*, 411, 66–69, <https://doi.org/10.1038/35075041>, 2001.
- Severmann, S., McManus, J., Berelson, W. M., and Hammond, D. E.: The continental shelf benthic iron flux and its isotope composition, *Geochim. Cosmochim. Ac.*, 74, 3984–4004, <https://doi.org/10.1016/j.gca.2010.04.022>, 2010.
- Shchepetkin, A. F.: An adaptive, Courant-number-dependent implicit scheme for vertical advection in oceanic modeling, *Ocean Model.*, 91, 38–69, <https://doi.org/10.1016/j.ocemod.2015.03.006>, 2015.
- Shchepetkin, A. F. and McWilliams, J. C.: The regional oceanic modeling system (ROMS): a split-explicit, free-surface, topography-following-coordinate oceanic model, *Ocean Model.*, 9, 347–404, <https://doi.org/10.1016/j.ocemod.2004.08.002>, 2005.
- Shiller, A. M., Gieskes, J. M., and Brian Price, N.: Particulate iron and manganese in the Santa Barbara Basin, California, *Geochim. Cosmochim. Ac.*, 49, 1239–1249, [https://doi.org/10.1016/0016-7037\(85\)90013-4](https://doi.org/10.1016/0016-7037(85)90013-4), 1985.
- Sholkovitz, E. and Soutar, A.: Changes in the composition of the bottom water of the Santa Barbara Basin: effect of turbidity currents, *Deep-Sea Res. Oceanogr. Abstr.*, 22, 13–21, [https://doi.org/10.1016/0011-7471\(75\)90014-5](https://doi.org/10.1016/0011-7471(75)90014-5), 1975.
- Sholkovitz, E. R. and Gieskes, J. M.: A PHYSICAL-CHEMICAL STUDY OF THE FLUSHING OF THE SANTA BARBARA BASIN: FLUSHING OF THE SANTA BARBARA BASIN, *Limnol. Oceanogr.*, 16, 479–489, <https://doi.org/10.4319/lo.1971.16.3.0479>, 1971.
- Sigman, D. M., Robinson, R., Knapp, A. N., van Geen, A., McCorkle, D. C., Brandes, J. A., and Thunell, R. C.: Distinguishing between water column and sedimentary denitrification in the Santa Barbara Basin using the stable isotopes of nitrate, *Geochem. Geophys. Geosys.*, 4, 1040, <https://doi.org/10.1029/2002GC000384>, 2003.
- Soetaert, K., Middelburg, J. J., Herman, P. M. J., and Buis, K.: On the coupling of benthic and pelagic biogeochemical models, *Earth-Sci. Rev.*, 51, 173–201, [https://doi.org/10.1016/S0012-8252\(00\)00004-0](https://doi.org/10.1016/S0012-8252(00)00004-0), 2000.
- Somes, C. J., Dale, A. W., Wallmann, K., Scholz, F., Yao, W., Oschlies, A., Muglia, J., Schmittner, A., and Achterberg, E. P.: Constraining global marine iron sources and ligand-mediated scavenging fluxes with GEOTRACES dissolved iron measurements in an ocean biogeochemical model, *Global Biogeochem. Cy.*, 35, 6948, <https://doi.org/10.1029/2021gb006948>, 2021.
- Sommer, S., Gier, J., Treude, T., Lomnitz, U., Dengler, M., Cardich, J., and Dale, A. W.: Depletion of oxygen, nitrate and nitrite in the Peruvian oxygen minimum zone cause an imbalance of benthic nitrogen fluxes, *Deep-Sea Res. Pt. I*, 112, 113–122, <https://doi.org/10.1016/j.dsr.2016.03.001>, 2016.
- Tagliabue, A., Sallée, J.-B., Bowie, A. R., Lévy, M., Swart, S., and Boyd, P. W.: Surface-water iron supplies in the Southern Ocean sustained by deep winter mixing, *Nat. Geosci.*, 7, 314–320, <https://doi.org/10.1038/ngeo2101>, 2014.
- Tagliabue, A., Aumont, O., DeAth, R., Dunne, J. P., Dutkiewicz, S., Galbraith, E., Misumi, K., Moore, J. K., Ridgwell, A., Sherman, E., Stock, C., Vichi, M., Völker, C., and Yool, A.: How well do global ocean biogeochemistry models simulate dissolved iron distributions?: GLOBAL IRON MODELS, *Global Biogeochem. Cy.*, 30, 149–174, <https://doi.org/10.1002/2015GB005289>, 2016.
- Tagliabue, A., Bowie, A. R., Boyd, P. W., Buck, K. N., Johnson, K. S., and Saito, M. A.: The integral role of iron in ocean biogeochemistry, *Nature*, 543, 51–59, <https://doi.org/10.1038/nature21058>, 2017.
- Testa, J. M., Brady, D. C., Di Toro, D. M., Boynton, W. R., Cornwell, J. C., and Kemp, W. M.: Sediment flux modeling: Simulating nitrogen, phosphorus, and silica cycles, *Estuar. Coast. Shelf S.*, 131, 245–263, <https://doi.org/10.1016/j.ecss.2013.06.014>, 2013.
- Till, C. P., Solomon, J. R., Cohen, N. R., Lampe, R. H., Marchetti, A., Coale, T. H., and Bruland, K. W.: The iron limitation mosaic in the California Current System: Factors governing Fe availability in the shelf/near-shelf region, *Limnol. Oceanogr.*, 64, 109–123, <https://doi.org/10.1002/lno.11022>, 2019.
- Treude, T. and Valentine, D. L.: Benthic fluxes of solutes measured by in-situ benthic flux chambers along two depth transects in the Santa Barbara Basin during November 2019 (Version 1), Biological and Chemical Oceanography Data Management Office (BCO-DMO) [data set], <https://doi.org/10.26008/1912/bco-dmo.896706.1>, 2023.
- Treude, T., Smith, C. R., Wenzhöfer, F., Carney, E., Bernardino, A. F., Hannides, A. K., Krüger, M., and Boetius, A.: Biogeochemistry of a deep-sea whale fall: sulfate reduction, sulfide efflux and methanogenesis, *Mar. Ecol.-Prog. Ser.*, 382, 1–21, 2009.
- Valentine, D. L., Fisher, G. B., Pizarro, O., Kaiser, C. L., Yoerger, D., Breier, J. A., and Tarn, J.: Autonomous Marine Robotic Technology Reveals an Expansive Benthic Bacterial Community Relevant to Regional Nitrogen Biogeochemistry, *Environ. Sci. Technol.*, 50, 11057–11065, <https://doi.org/10.1021/acs.est.6b03584>, 2016.
- Wallmann, K., José, Y. S., Hopwood, M. J., Somes, C. J., Dale, A. W., Scholz, F., Achterberg, E. P., and Oschlies, A.: Biogeochemical feedbacks may amplify ongoing and future ocean deoxygenation: a case study from the Peruvian oxygen minimum zone, *Biogeochemistry*, 159, 45–67, <https://doi.org/10.1007/s10533-022-00908-w>, 2022.
- White, M. E., Rafter, P. A., Stephens, B. M., Wankel, S. D., and Aluwihare, L. I.: Recent Increases in Water Column Denitrification in the Seasonally Suboxic Bottom Waters of the Santa Barbara Basin, *Geophys. Res. Lett.*, 46, 6786–6795, <https://doi.org/10.1029/2019GL082075>, 2019.
- Widdows, J. and Brinsley, M.: Impact of biotic and abiotic processes on sediment dynamics and the consequences to the structure and functioning of the intertidal zone, *J. Sea Res.*, 48, 143–156, [https://doi.org/10.1016/S1385-1101\(02\)00148-X](https://doi.org/10.1016/S1385-1101(02)00148-X), 2002.
- Yao, M., Henny, C., and Maresca, J. A.: Freshwater Bacteria Release Methane as a By-Product of Phosphorus Acquisition, *Appl. Environ. Microb.*, 82, 6994–7003, <https://doi.org/10.1128/AEM.02399-16>, 2016.
- Yousavich, D. J., Robinson, D., Peng, X., Krause, S. J. E., Wenzhöfer, F., Janssen, F., Liu, N., Tarn, J., Kinnaman, F., Valen-

tine, D. L., and Treude, T.: Marine anoxia initiates giant sulfur-oxidizing bacterial mat proliferation and associated changes in benthic nitrogen, sulfur, and iron cycling in the Santa Barbara Basin, California Borderland, *Biogeosciences*, 21, 789–809, <https://doi.org/10.5194/bg-21-789-2024>, 2024.

Zhou, Y., Gong, H., and Zhou, F.: Responses of Horizontally Expanding Oceanic Oxygen Minimum Zones to Climate Change Based on Observations, *Geophys. Res. Lett.*, 49, e2022GL097724, <https://doi.org/10.1029/2022GL097724>, 2022.